

Harbin Institute of Technology

Design and Analysis of MEMS-based direct methanol fuel cell

Yuan Zhenyu

Harbin Institute of Technology

2010.10



Contents



Background

Principle

Application of COMSOL

Summary



Harbin Institute of Technology Background

Due to the unique advantages, micro direct methanol fuel cells (μ DMFCs) have been considered as the most promising candidates for the micro power sources of mobile devices.



μ DMFC for *speaker and gadget charger*, **Sony (Japan)**, 2009



μ DMFC for *cell phone*, **Motorola (USA)**, 2008



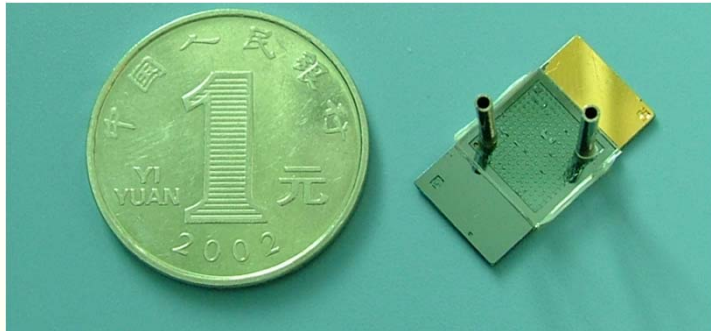
μ DMFC for *notebook*, **Ultracell (USA)**, 2007



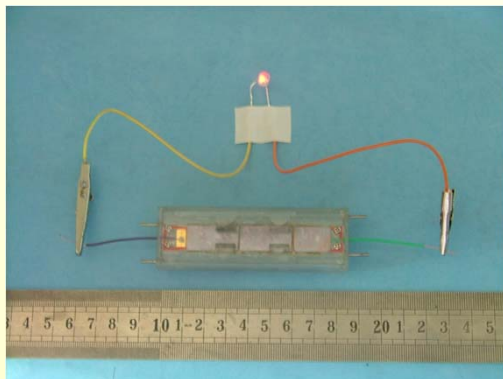
μ DMFC for *PDA*, **Hitachi (Japan)**, 2005



MEMS Center, HIT



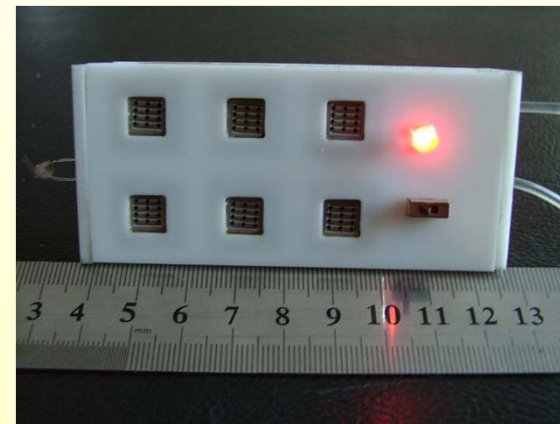
0.64cm², open circuit voltage:520mV, power density:5.9mW/cm²



fuel cell stack, open voltage:2.75V,
power density:6.8mW.



Open voltage:650mV
power density:15.9mW/cm²



Powered LED to work for 5h

contents



Background

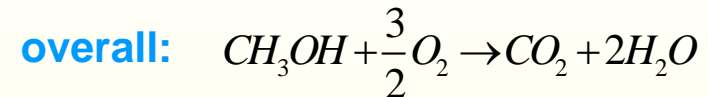
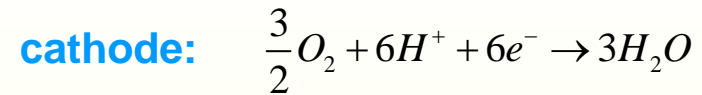
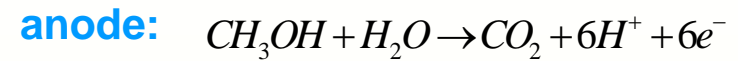
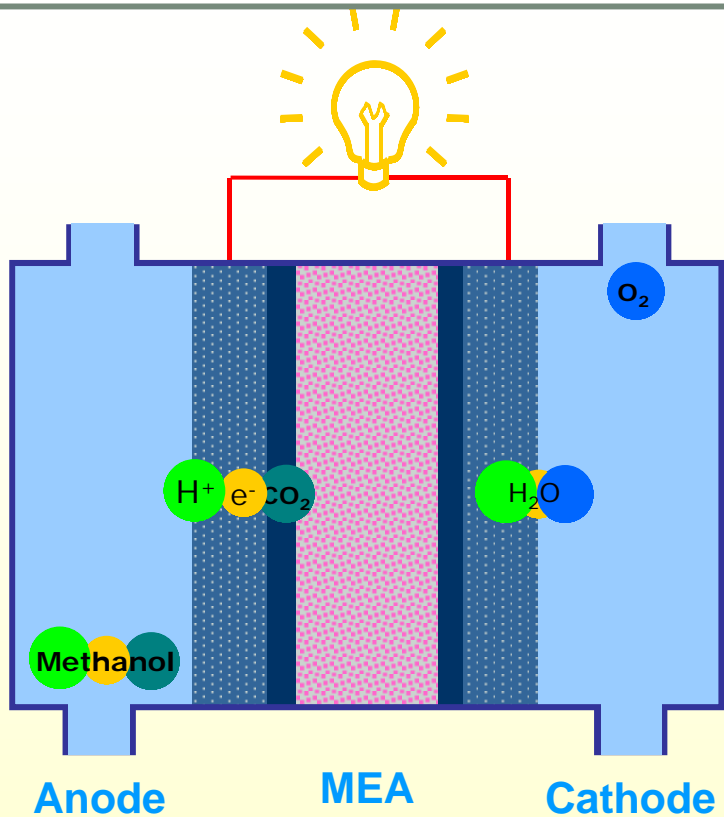
Principle

Application of COMSOL

Summary



Principle



- (1) current collector material
- (2) structure design
- (3) mass transfer of MEA
- (4) theoretical analysis

**COMSOL
Multiphysics**



contents



Background

Principle

Application of COMSOL

Summary

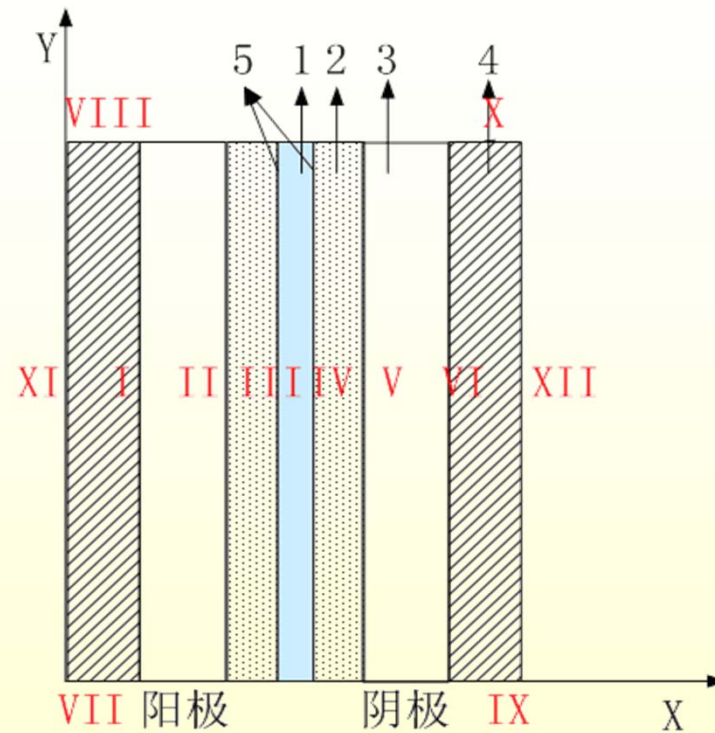


3. Application of COMSOL

- 3.1 Two-dimensional, two-phase mass transport——mass transport, **structure of DMFC**
- 3.2 μ DMFC Three-dimensional model
- A novel cathode——**structure**, stability
- A air-breathing cathode flow field——**water-flooding**
- Anode structure ——**optimize structure**



3.1A two-dimensional two-phase mass transport model :



- 1—质子交换膜 2—气体扩散层 3—流道
- 4—电流收集层 5—催化层



Mathematical model

► two-phase mass transport in the diffusion layer

• continuous equation

$$\begin{cases} \nabla \cdot (\rho_l \mathbf{u}_l) = S_l \\ \nabla \cdot (\rho_g \mathbf{u}_g) = S_g \end{cases}$$

• momentum transport equation

$$\begin{cases} \mathbf{u}_l = \frac{-Kk_{rl}}{\mu_l} \nabla p_l & k_{rl} = s^3 \\ \mathbf{u}_g = \frac{-Kk_{rg}}{\mu_g} \nabla p_g & k_{rg} = (1-s)^3 \end{cases}$$

• Mass transport equation

$$\begin{cases} \nabla \cdot (-D_{i,l}^{eff} \nabla C_{i,l} + C_{i,l} \mathbf{u}_l) = S_{i,l} & D_{i,l}^{eff} = D_{i,l} \varepsilon^{1.5} s^{1.5} \\ \nabla \cdot (-D_{i,g}^{eff} \nabla C_{i,g} + C_{i,g} \mathbf{u}_g) = S_{i,g} & D_{i,g}^{eff} = D_{i,g} \varepsilon^{1.5} (1-s)^{1.5} \end{cases}$$

• pressure difference $p_c = p_g - p_l = \sigma \cos \theta_c (\varepsilon / K)^{0.5} J(s)$

$$\text{Leverette function } J(s) = \begin{cases} 1.417(1-s) - 2.120(1-s)^2 + 1.263(1-s)^3 & 0 < \theta_c < 90^\circ \\ 1.417s - 2.120s^2 + 1.263s^3 & 90^\circ < \theta_c < 180^\circ \end{cases}$$



Mathematical model

➤ two-phase mass transport in anode channel

• momentum transport equation
$$\frac{\partial(\phi\rho_l\mathbf{u}_l)}{\partial t} + \nabla \cdot (\phi\rho_l\mathbf{u}_l\mathbf{u}_l) = -\nabla p_l + \nabla \cdot (\phi\mu_l\nabla\mathbf{u}_l) + \phi\rho_l\mathbf{g}$$

CO₂ velocity —
$$\mathbf{u}_g = \mathbf{u}_l + \mathbf{u}_{slip} \quad \frac{3}{4} \frac{C_d}{d_b} \rho_l |\mathbf{u}_{slip}| \mathbf{u}_{slip} = -\nabla p_l \quad C_d = \frac{16}{\text{Re}_b}$$

• continuous equation
$$\begin{cases} \nabla \cdot (\phi\rho_l\mathbf{u}_l) = 0 \\ \frac{\partial((1-\phi)\rho_{CO_2})}{\partial t} + \nabla \cdot ((1-\phi)\rho_{CO_2}\mathbf{u}_g) = 0 \end{cases}$$

• Mass transport of methanol —
$$\nabla \cdot (-D_{MeOH}^{eff} \nabla C_{MeOH} + C_{MeOH}\mathbf{u}_l) = 0 \quad D_{MeOH}^{eff} = D_{MeOH}\phi^{1.5}$$

➤ two-phase mass transport in cathode channel

• momentum transport equation —

$$\frac{\partial((1-\phi)\rho_g\mathbf{u}_g)}{\partial t} + \nabla \cdot ((1-\phi)\rho_g\mathbf{u}_g\mathbf{u}_g) = -\nabla p_g + \nabla \cdot ((1-\phi)\mu_g\nabla\mathbf{u}_g) + (1-\phi)\rho_g\mathbf{g}$$

H₂O velocity —
$$\mathbf{u}_g = \mathbf{u}_l \quad \begin{cases} \nabla \cdot ((1-\phi)\rho_g\mathbf{u}_g) = 0 \\ \frac{\partial(\phi\rho_{H_2O})}{\partial t} + \nabla \cdot (\phi\rho_{H_2O}\mathbf{u}_l) = 0 \end{cases}$$

• continuous equation

• Mass transport of O₂ —
$$\nabla \cdot (-D_{O_2}^{eff} \nabla C_{O_2} + C_{O_2}\mathbf{u}_g) = 0 \quad D_{O_2}^{eff} = D_{O_2}(1-\phi)^{1.5}$$



Mathematical model

► mass transport in PEM

- Mass transport of methanol (Concentration and electro-osmotic) —

$$N_{MeOH,cross} = -D_{MeOH,mem}^{eff} \nabla C_{MeOH,mem} + n_d^m \frac{i}{F} = \frac{i_p}{6F}$$

- Mass transport of H₂O — $N_{H_2O,cross} = n_d \frac{i}{F}$

► The transportations of electron and proton

$$\nabla \cdot (\sigma_{s,eff} \nabla \phi_s) = 0 \qquad \nabla \cdot (\sigma_{m,eff} \nabla \phi_m) = 0$$

► Electrochemical kinetics

- Anode —
$$i = i_m^{ref} s \left(\frac{C_{m,acl}}{C_m^{ref}} \right)^\gamma \exp\left(\frac{\alpha_a F}{RT_{acl}} \eta_a\right) \quad \gamma = \begin{cases} 0 & C_{m,acl} > C_m^{ref} \\ 1 & C_{m,acl} \leq C_m^{ref} \end{cases} \quad C_m^{ref} = 0.1 \text{ mol} / L$$

- Cathode —
$$i_c = i_{O_2}^{ref} (1-s) \frac{C_{O_2,ccl}}{C_{O_2}^{ref}} \exp\left(-\frac{\alpha_c F}{RT_{ccl}} \eta_c\right)$$

- Current density —
$$i_p = i_c - i$$

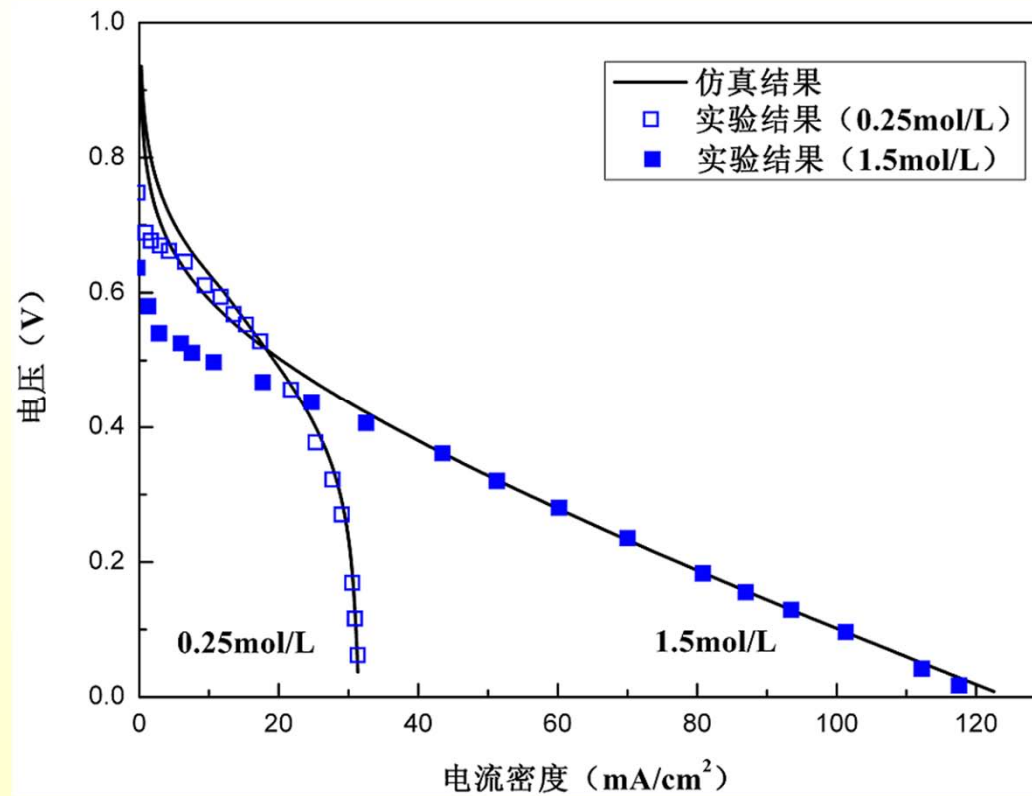
► Heat transfer

- Anode catalyst layer —
$$q_{acl} = i_a \left(\eta_a - \frac{\Delta H_a - \Delta G_a}{6F} \right)$$

- Cathode catalyst layer —
$$q_{ccl} = i_c \left(\eta_c - \frac{\Delta H_c - \Delta G_c}{4F} \right) - (i_c - i_a) \frac{\Delta H_a - \Delta G_a}{6F}$$



➤ Comparison of the modeling results and experimental results



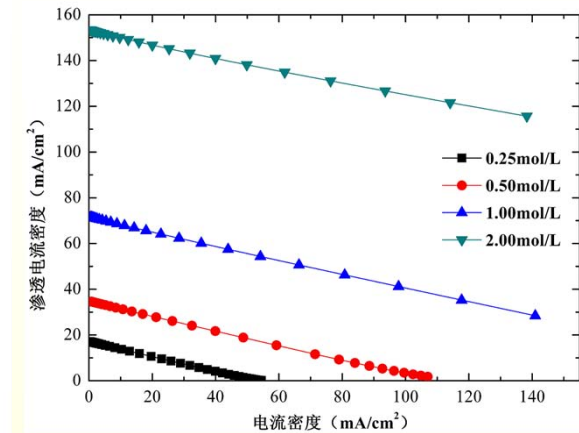
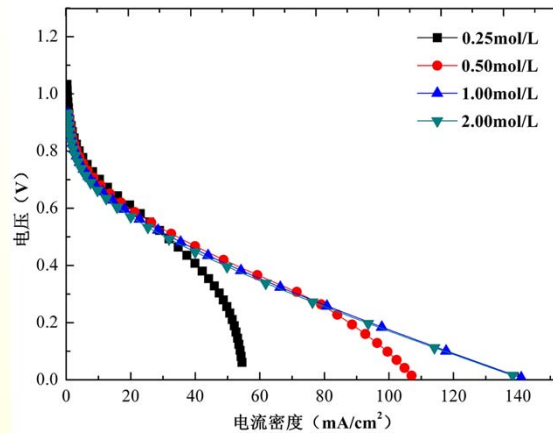
Model result

diffusion

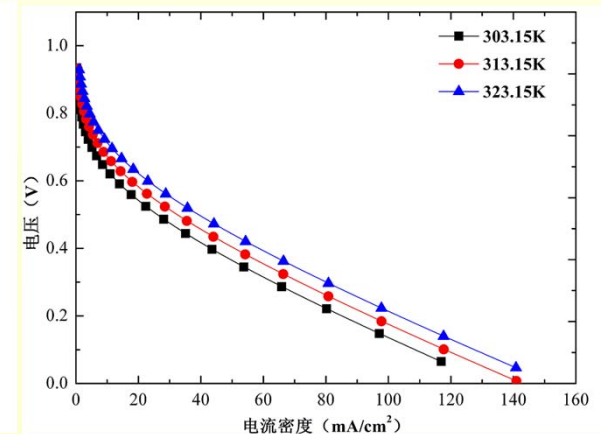
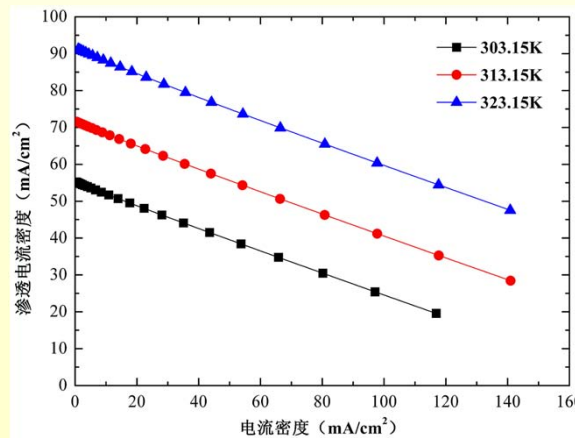
electroosmosis

➤ effect of different methanol concentrations

$$N_{MeOH,cross} = -D_{m,mem}^{eff} \nabla C_{m,mem} + n_d^m \frac{i}{F} = \frac{i_p}{6F}$$



➤ Effect of the operating temperature



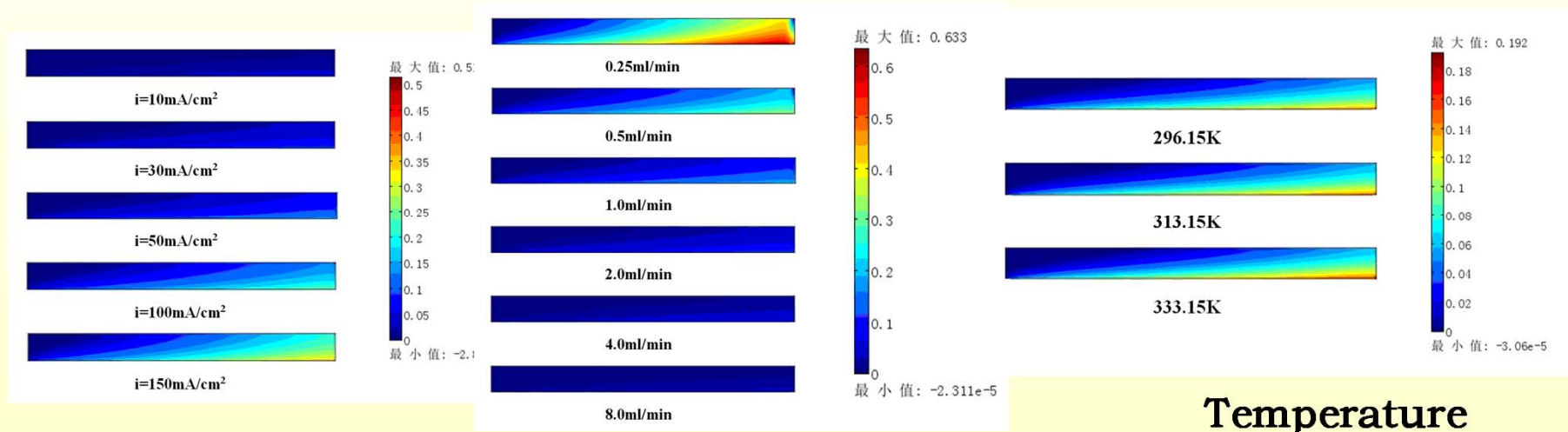
Model result

➤ CO₂ content in anode flow field

- CO₂ content increase with the current density and temperature
- The anode flow rates have the effect of the removal rate of the CO₂
- in accord with the results of Yang^[1] and Liao^[2]

[1] H. Yang, T. S. Zhao, Q. Ye. J. Power Sources, 2005, 139: 79-90

[2] Q. Liao, X. Zhu, X. Y. Zheng, et al. J. Power Sources, 2007, 171: 644-651



Current density

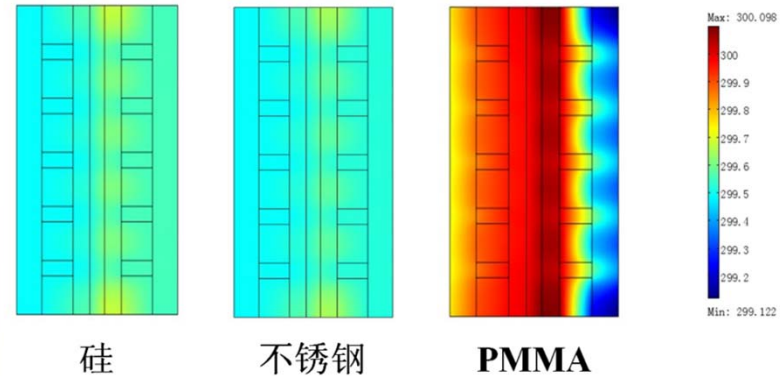
Flow rate

Temperature



Simulation Result

Temperature distribution in the μ DMFC with different current collector materials : (a) silicon; (b) stainless steel; (c) PMMA.

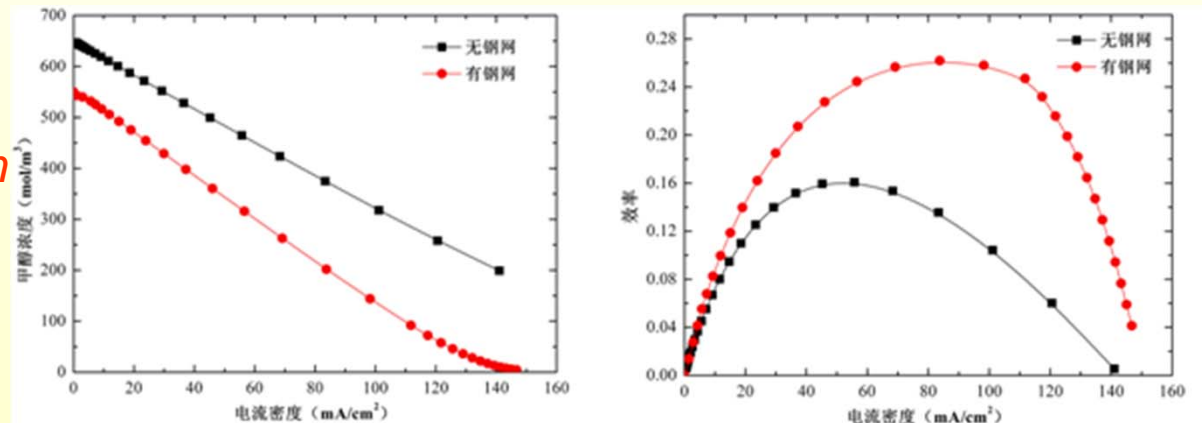


excellent qualities of the silicon and stainless steel in heat transfer, uniform temperature distributions were achieved in their corresponding cells

•stainless steel mesh

smaller methanol concentration in the anode catalyst layer, obtain the better performance

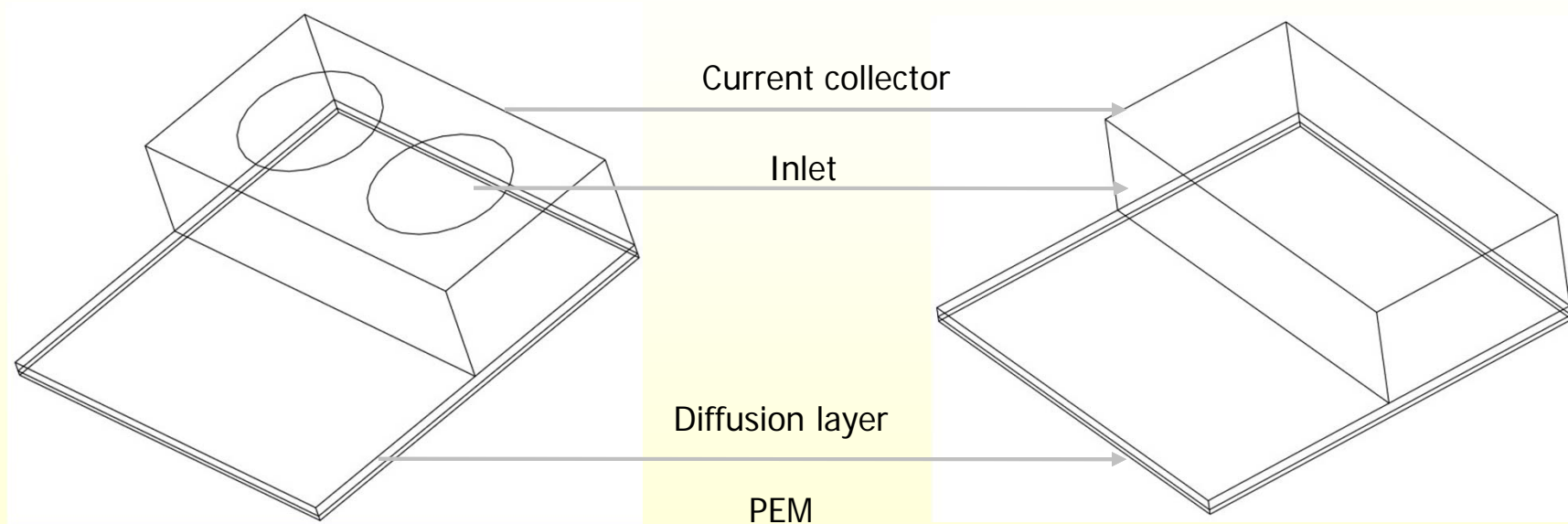
$$\eta = \eta_{th} \eta_{volt} \eta_{fuel} = \frac{\Delta G}{\Delta H} \times \frac{V_{cell}}{E_{cell}} \times \frac{i_a}{i_c} \times 100\%$$



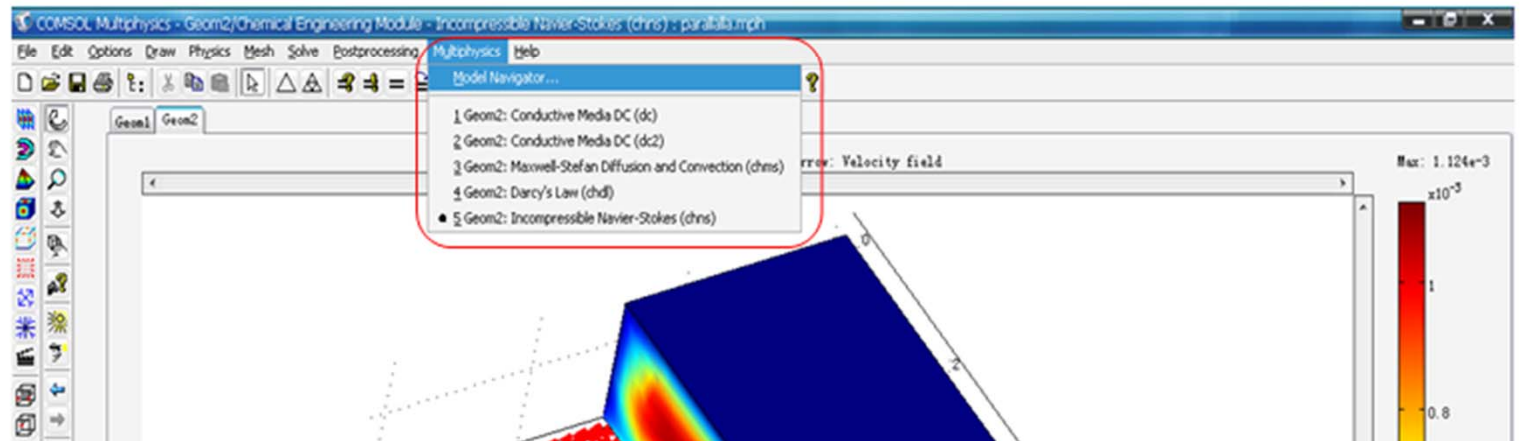
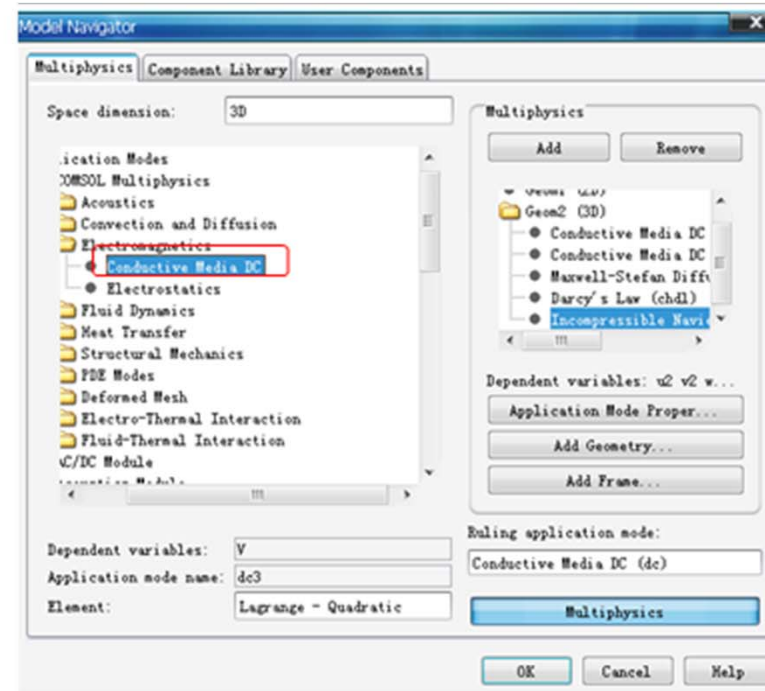
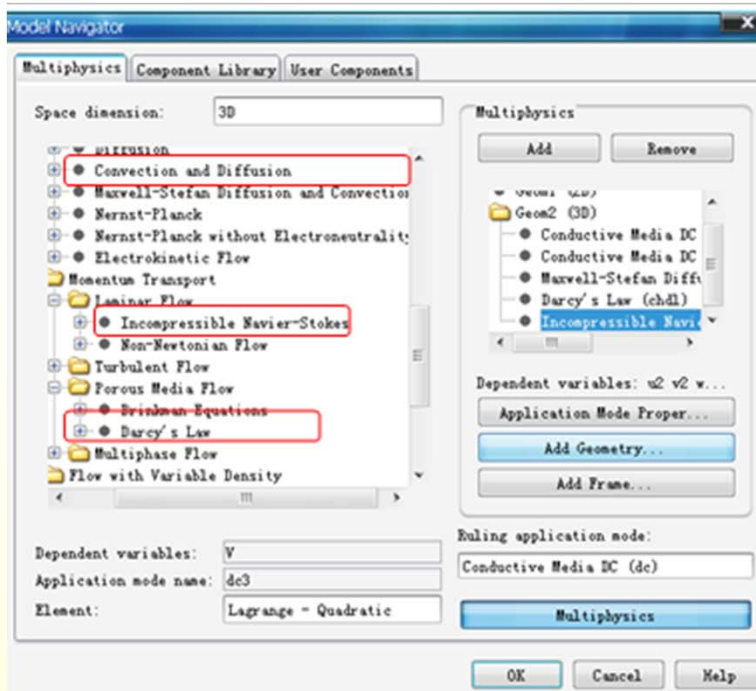
•Journal of Power Sources 195 (2010) 7338 – 7348 (IF=3.792)

3.2 μ DMFC three-dimensional Model

3.2.1 An air-breathing direct methanol fuel cell with a novel cathode shutter current collector



Harbin Institute of Technology

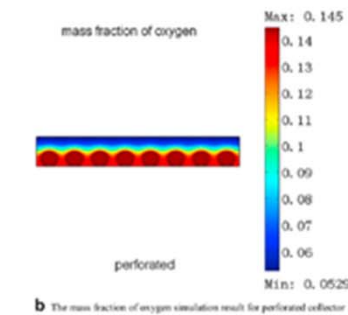
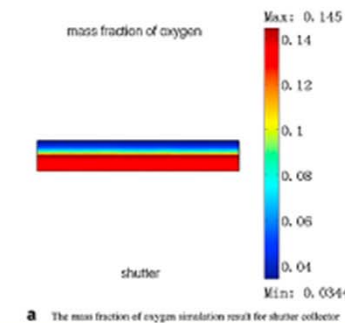
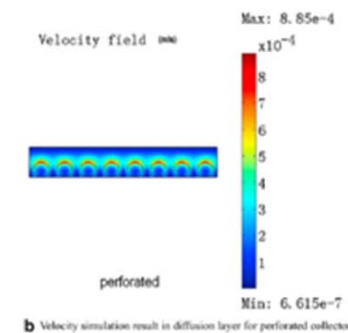
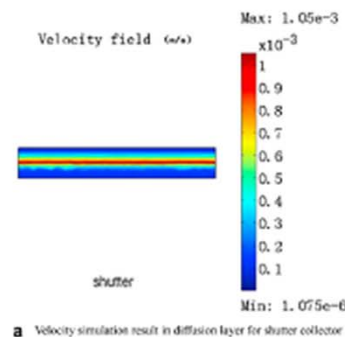
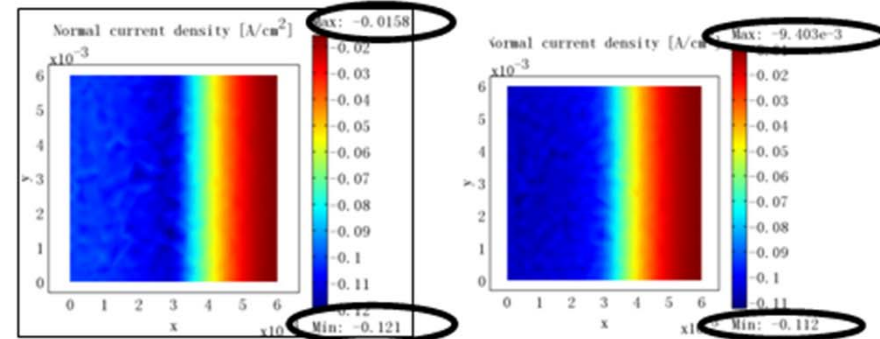


The velocity simulation results in diffusion layer with two types of collectors.

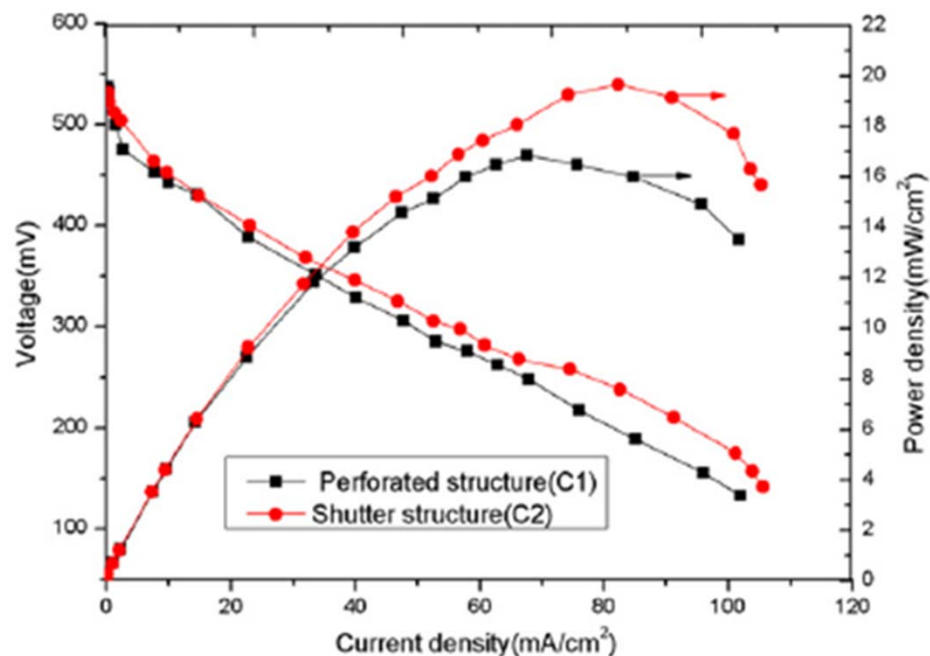
The mass fraction of oxygen simulation results with the two types of collector.

百叶窗结构

多孔结构



Test result



All experiments of the stack were performed with air self-breathing at room temperature on the cathode. Flow rates of 2 mL/min for 2 M methanol solution were supplied by a peristaltic pump.

international journal of hydrogen energy 35 (2010) 5638-5646(IF=3.945)

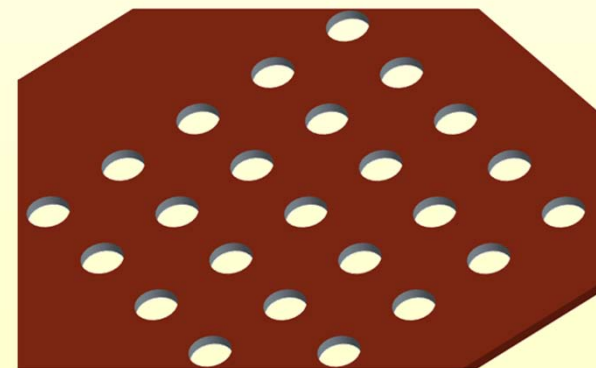
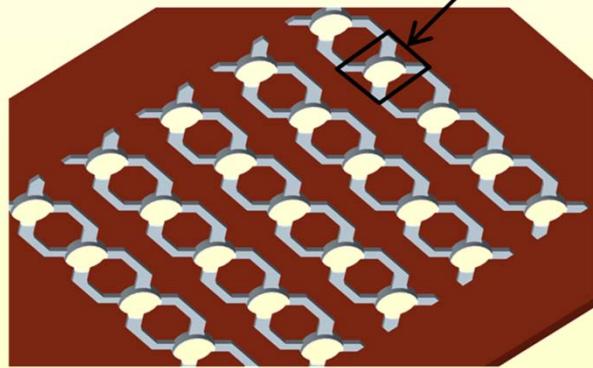


3.2.2a three-dimensional two-phase-flow model for self-breathing μ DMFCs

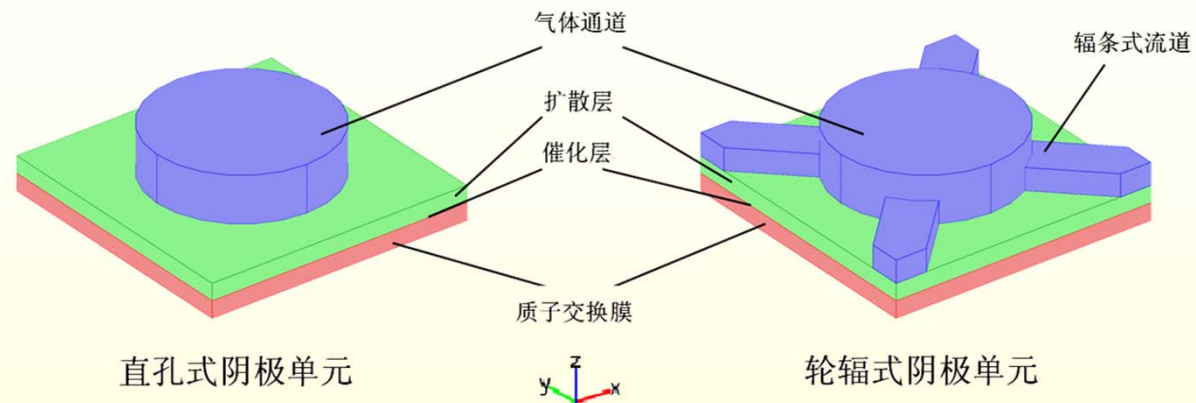
In order to ensure that the oxygen from air could enter the electrochemical reaction sufficiently and is well-distributed, the intension of this paper is to design a self-breathing μ DMFC with a new cathode spoke structure

➤ structure

a similar back interface (air-contacting interface) structure to conventional perforated cathode, its front interface (electrode-contacting interface) is equipped with a certain number of blade-form channels which are connected with self-breathing circular openings to form a “spoke” unit.



➤ Schematic of simulation domains of the three-dimensional model



➤ Governing equations

• **electronic current** — $-\nabla(-\sigma_{l,eff} \nabla \phi_l) = -S_a i_c$ $-\nabla(-\sigma_{s,eff} \nabla \phi_s) = S_a i_c$

• **Multicomponent mixed gas diffusion** — $\pi_i = \left\{ -\rho_g w_i \sum_{j=1}^3 \frac{MD_{ij}}{M_j} (\nabla w_j + \frac{w_j}{M} \nabla M) + w_i \rho \right.$

(Maxwell-Stefan)



➤ Governing equations

- oxygen concentration — $\nabla \cdot (-D\nabla c_{O_2}) = R - \mathbf{u}_g \cdot \nabla c_{O_2}$

- mass transport equation of the liquid-phase

$$-\nabla \cdot \left(-\frac{\rho_l}{M_l} \frac{Kk_{rl}}{\mu_l} \sigma \cos(\theta_c) \left(\frac{\varepsilon}{K} \right)^{0.5} \nabla J(s) \right) + R_w = 0$$

- The gas flow in the cathode flow channel is expressed by N-S equation:

$$\rho_g \frac{\partial \mathbf{u}_g}{\partial t} - \nabla \cdot \mu_g (\nabla \mathbf{u}_g + (\nabla \mathbf{u}_g)^T) + \rho_g (\mathbf{u}_g \cdot \nabla) \mathbf{u}_g + \nabla p_c = 0$$

- The gas velocity in the diffusion layer $\mathbf{u}_g = -\frac{Kk_{rg}}{\mu_g} \nabla p_g$

- Butler-Volmer equation is used for explaining the relation between current and potential:

$$i_c = i_0 \left(\frac{c_{O_2}}{c_{O_2,ref}} \right) \exp\left(-\frac{\alpha_c F (\phi_s - \phi_l)}{RT_0} \right)$$



Result and discussion

➤ compare of different cahtode

•increases the efficiency of oxygen mass transport

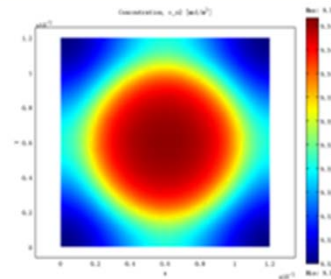
make the concentration more equal

•promotes the water transfer to PEM

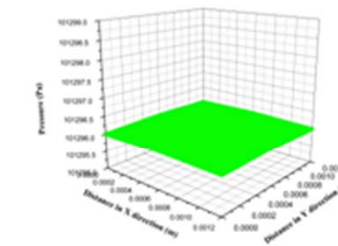
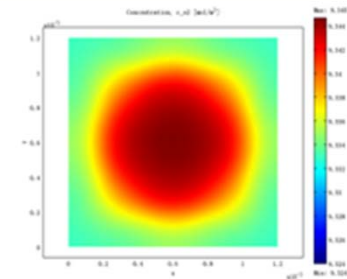
• declining the inner resistance among PEM

•Enchancing Electrocatalytic Activity

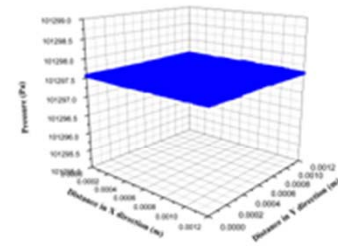
•Promoting the air vaporization



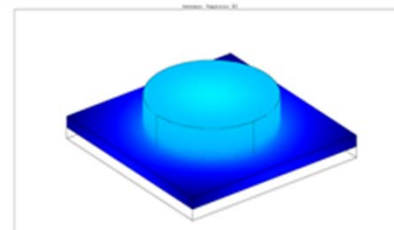
perforated (concentration) spoke



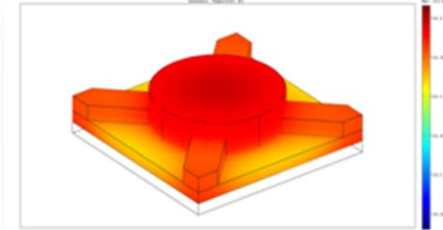
perforated (pressure)



spoke



perforated (temperature)

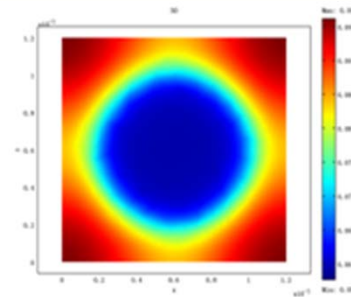


spoke

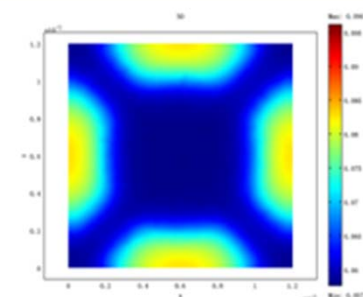


➤ compare of different cahtode

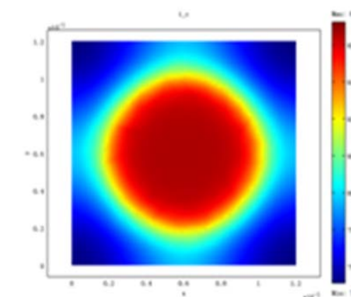
- The latter shows a lower content than the former
- indicating a higher discharge capability



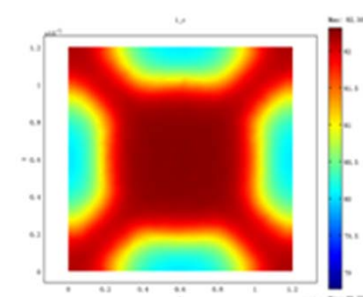
perforated (saturation)



spoke



perforated (current)



spoke

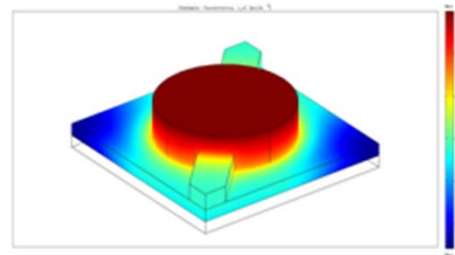


Model result

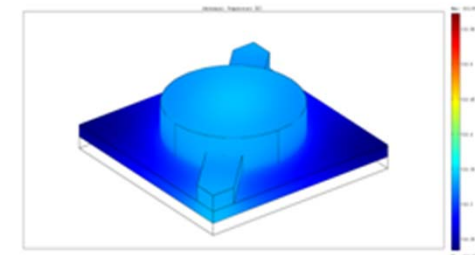
➤ different numbers of blades

- the eight-blade cathode shows the highest
- The distributions of the four-blade and the eight-blade are relatively uniform

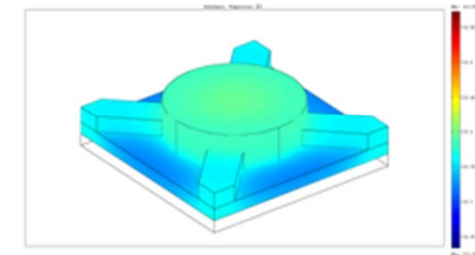
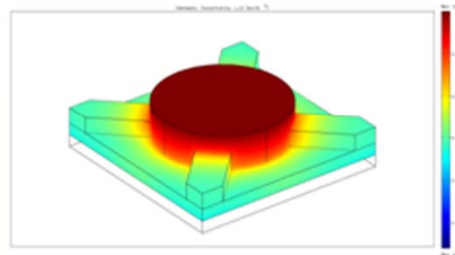
(oxygen concentration)



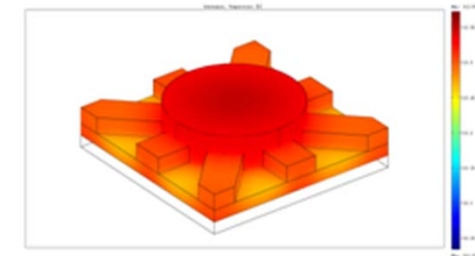
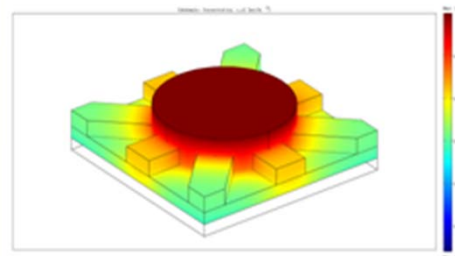
(temperature)



(two-blade)



(four-blade)

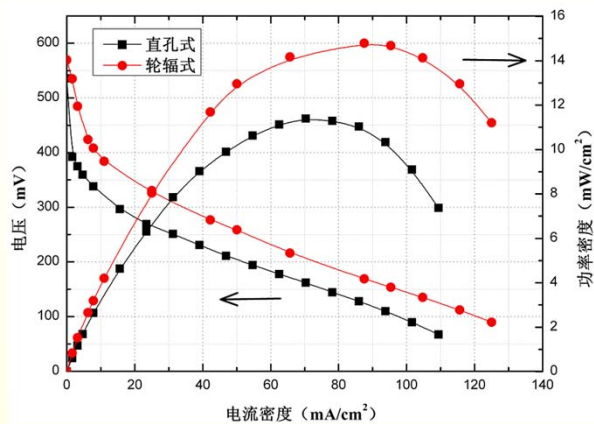


(eight-blade)

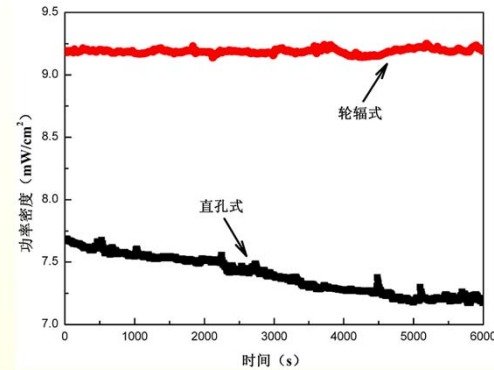


Test result

➤ cathode structure



Performance comparison



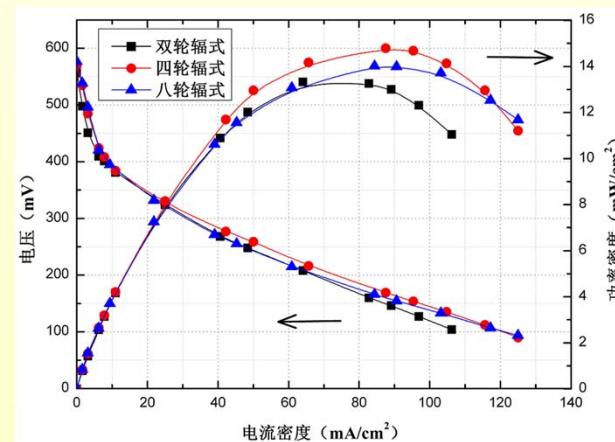
Durability

➤ number of blade

two-blade — 13.33 mW/cm²

four-blade — 14.79 mW/cm²

eight-blade — 14.01 mW/cm²

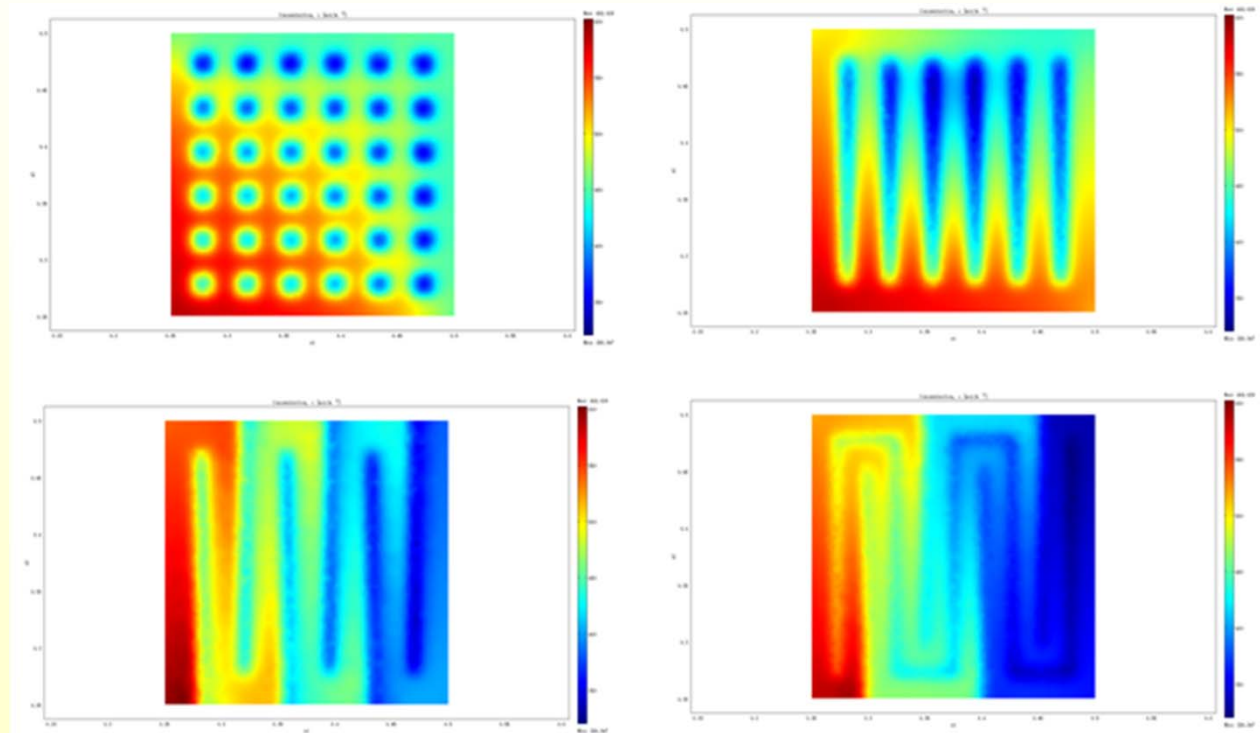


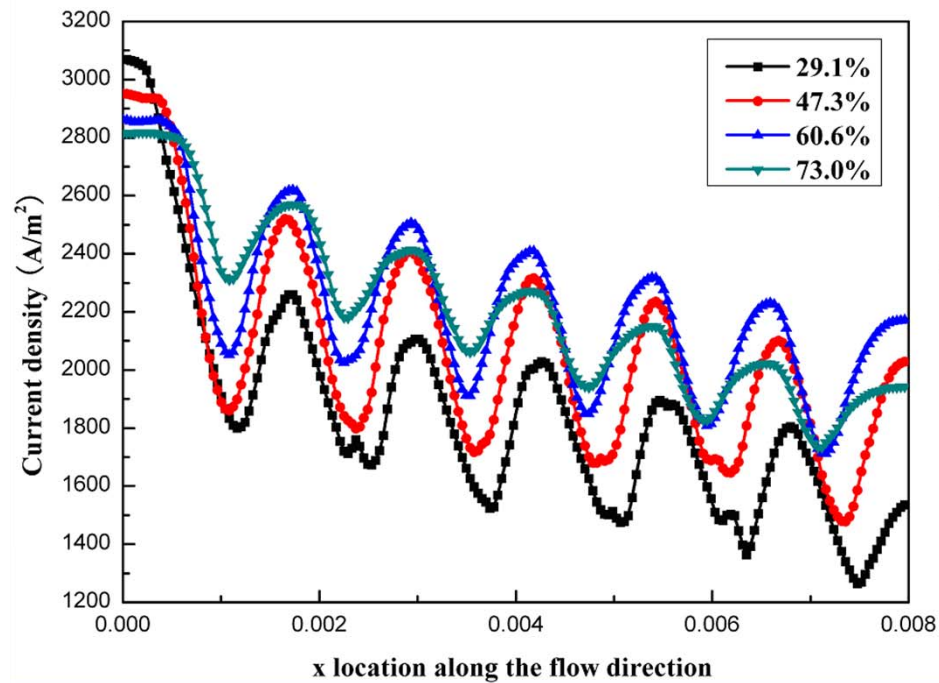
Performance comparison



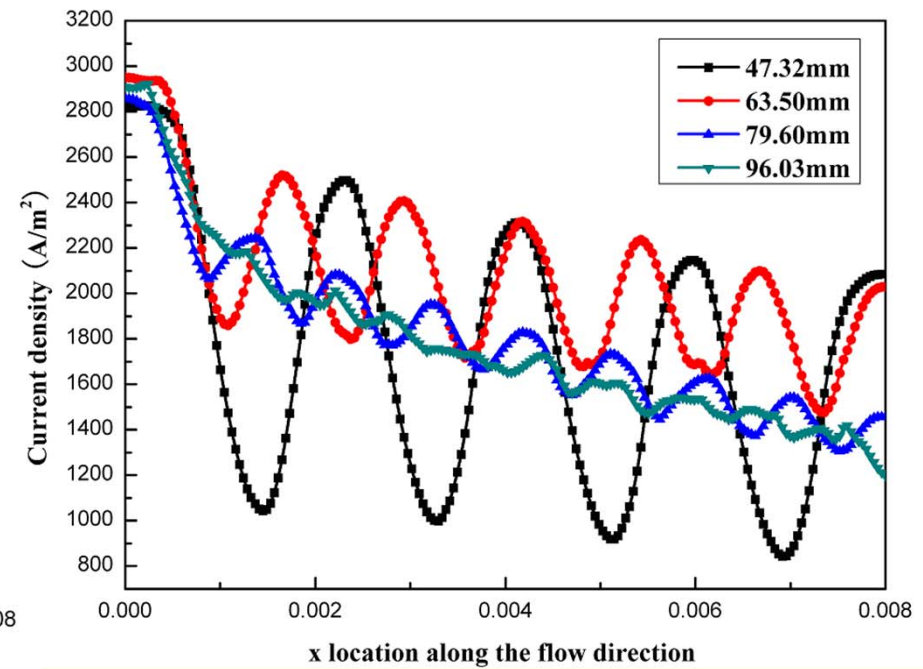
Methanol concentration distributions at the catalyst layers under different flow fields are 586.58、585.29、602.03和590.93mol/m³

single serpentine field flow has best performance



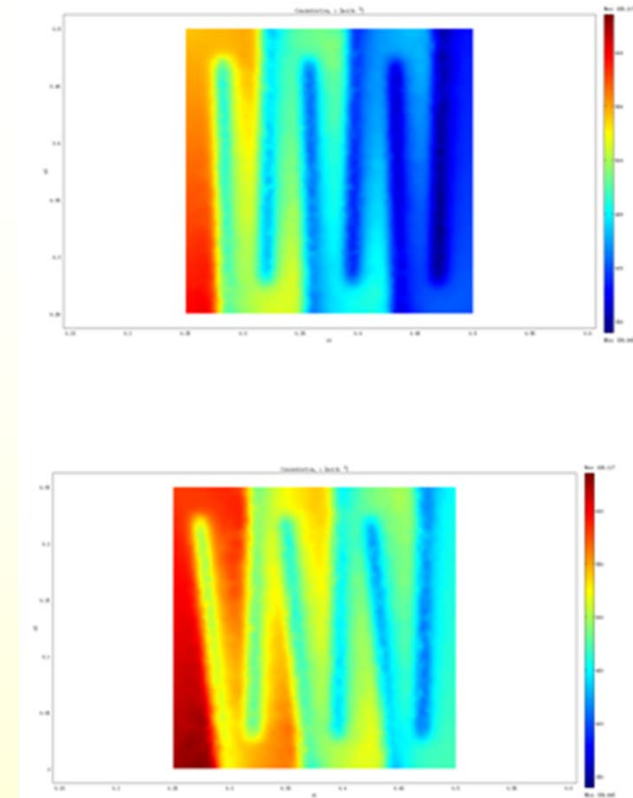
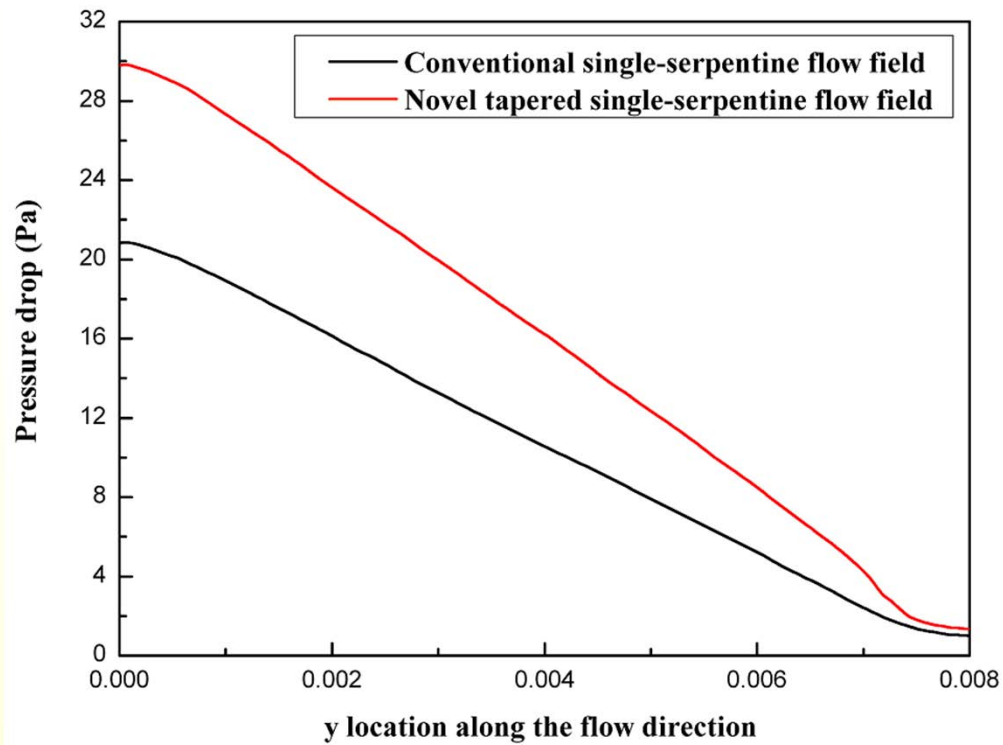


Current density distributions at the catalyst layers along x direction under the conditions of different open ratios.



Current density distributions at the catalyst layers along x direction under the conditions of different channel depth.





Comparison of the line pressure drop at the interfaces between the diffusion layers and two single-serpentine flow fields

Methanol concentration distributions



contents



Background

Principle

Application of COMSOL

Summary



4. summary

outlook:

- **Methanol crossover**
- **Analyses of the fuel cell stack assembly pressure**



THANKS!

